

## A study on the structural performance of new shape built-up square column under concentric axial load

Sun-Hee Kim <sup>1a</sup>, Kyong-Soo Yom <sup>2b</sup> and Sung-Mo Choi <sup>\*1</sup>

<sup>1</sup> Department of Architectural Engineering, University of Seoul,  
Cheonnong-dong 90, Dongdaemun-Gu, Seoul, 130-743, Republic of Korea

<sup>2</sup> Harmony Engineering, Guro-Gu Seoul 152-051, Republic of Korea

(Received June 30, 2014, Revised September 19, 2014, Accepted December 01, 2014)

**Abstract.** Recently, in recognition of their outstanding structural performance, the use of Concrete Filled Steel Tube (CFT) columns has been increased. New shape welded built-up square tube was developed by the authors for broader usability using thin steel plates which were bent to be L-shaped (Channel) and each unit members were welded to form square steel tube as an cost-efficient use of expensive steel. In addition, since the rib placed at the center of the tube width acts as an anchor; higher load capacity of buckling is achievable. In order to apply the new shape built-up square columns, the structural behavior and stress distribution with parameter width of thickness ( $b/t$ ), with and without rib were predicted. The New shape welded built-up square tube effectively delayed the local buckling of the steel tube, which led to a greater strength and ductility than regular HSS.

**Keywords:** built-up square column; composite effect; width of thickness; concentric axial load

### 1. Introduction

#### 1.1 Background

The study on the concrete-filled columns where two construction materials act as one structure has been continuously conducted since the late 1990s (Furlong 1967, Tomii and Sakino 1979, Uy and Bradford 1996, Hajjar and Gourley 1996). Having advantages over other structural systems in terms of structural performance, design and workability, they have been widely acknowledged and employed worldwide. The biggest structural advantage of the column lies in the fact that the steel tube restrains the lateral displacement of the concrete and forms 3-axis stress condition of the concrete, which enables the confinement effect to improve strength and ductility. In addition, the concrete inside the steel tube delays its local buckling (Park and Paulay 1933, Schneider 1998). Nevertheless, the rise in steel price has called for the use of CFT columns fabricated from thin steel plates (Xiamuxi and Hasegawa 2011, Bahrami *et al.* 2011). However, the deterioration in the concrete confinement effect caused by the local buckling of the steel tubes is inherent in the CFT

---

\*Corresponding author, Professor, E-mail: [smc@uos.ac.kr](mailto:smc@uos.ac.kr)

<sup>a</sup> Ph.D., Research Professor, E-mail: [sun@uos.ac.kr](mailto:sun@uos.ac.kr)

<sup>b</sup> President, E-mail: [yks100nav@naver.com](mailto:yks100nav@naver.com)

columns fabricated with thin steel plates due to increased width-thickness ratio (Fujimoto *et al.* 2004). In an attempt to solve the problem, the columns with interior stiffeners were suggested to delay the local buckling of the columns having larger width-thickness ratio. Fig. 1(b) shows the sectional shape of the suggested columns (Lee *et al.* 2010, 2011). The new shape columns are made by cold-forming thin steel plates and welding the single bent steel plates. Recognized as a new technology in Korea, it is being increasingly employed in construction field. It is cost-effective because thin plates are used and the efficiency of the composite members is maximized thanks to the anchor effect between the stiffeners and the concrete. In this study, the shape shown in Fig. 1(c) is suggested to extend the range of the application of the new shape built-up square columns and their performance and behavior are examined through structural test and analysis.

### 1.2 Fabric-ability

The ACT (Advanced Construction Technology) tubes were produced with fabric-ability, practice and the design code in Korea taken into consideration. Each of the ACT tubes was fabricated from mild steel plates with a thickness of 3.2 mm. L-shaped unit members as shown in Fig. 2(a) were produced by cold-forming the steel plates. The internal radius of the unit member was 12 mm. The rib was bent at a 70 degree angle rather than a right angle to provide better composite effect between the steel tube and the concrete. The length from the internal face of the unit member to the end of the rib was 50 mm, which was the minimum length needed for the bending machine to grab and bend the steel plate. Four unit members were welded together to produce one ACT tube as shown in Fig. 2(b). The welding was performed using the shielded metal arc welding (SMAW) process for flare groove welds.

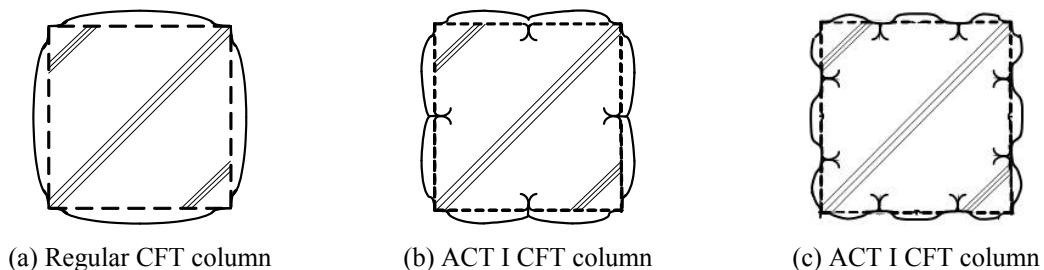


Fig. 1 Idealized local buckling mode

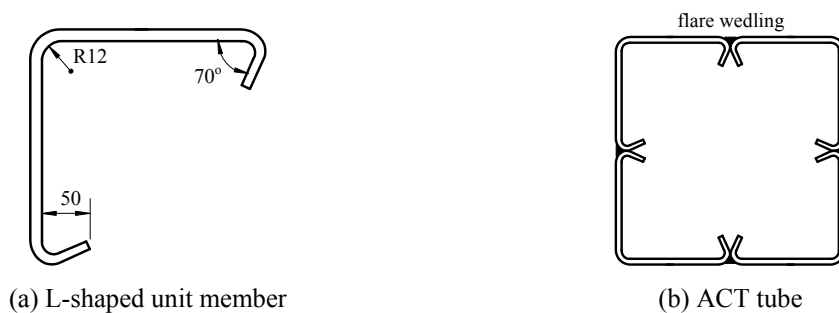


Fig. 2 Fabrication of ACT tube

## 2. Experimental program

### 2.1 Outline

In this study, width-thickness ratio ( $B/t$ ) was the main parameter to find out the deterioration in load capacity caused by the stiffeners. Width-thickness ratio of 57 is obtained as its limit by applying 325 MPa, the nominal yield strength ( $F_y$ ) of SM490 which is widely used in construction field as a column member, to current code (KBC 2005, 2009, AISC 2005, 2010). However, the specimens in this study were fabricated from SS400 because its actual yield strength is approximately 300 MPa, which is the nominal yield strength of SM490. Width-thickness ratios of 78, 96 and 107 were selected as parameters based on the limit of 57 imposed to SM490. Meanwhile, In AISC 2010 proposes a strength formula ( $P_{no}$ ) classified into compact, Non-compact and slender section element width thickness ratio as shown in Table 1. Width-thickness of all specimens is higher than in the non-compact section and satisfied with the maximum permitted range. The Compressive Strength is shown is equation (1) with slender section element ( $\lambda_m$ ). The elastic local buckling stress ( $F_{cr}$ ) from the plate buckling equation simplifies. As a result, Predicted by Eq (1) is estimated compressive strength of each specimen. Planned specimens were summarized in Table 2.

$$P_{no} = F_{cr} A_s + 0.7 f_c' \left( A_c + \left( \frac{A_{sr} E_s}{E_c} \right) \right) \tag{1}$$

Here, For rectangular filled sections  $F_{cr} = 9 \frac{E_s}{(b/t)}$

Table 1 Limiting width-to thickness ratio for compression in composite members

Description of element	$\lambda_p$	$\lambda_r$	Maximum permitted ( $\lambda_m$ )
Rectangular HSS and boxes of uniform thickness ( $b/t$ )	$2.26\sqrt{E/F_y}$	$3.00\sqrt{E/F_y}$	$5.00\sqrt{E/F_y}$
Round HSS ( $D/t$ )	$0.15E/F_y$	$0.19E/F_y$	$0.31E/F_y$

Table 2 Specimen details and expected strength

Specimens	Shape	$L$ (mm)	$B$ (mm)	$bc$ (mm)	$Be$ (mm)	$t$ (mm)	$B/t$	$P_{no}$ Eq. (1) (kN)
A0C78	Regular CFT	892	255	-	-	-	78	2759
A0C96		1102	315	-	-	-	96	3525
A0C107		1225	350	-	-	-	107	4099
A1C78	ACT I	892	255	-	-	3.2	78	2850
A1C96		1102	315	-	-		96	3580
A1C107		1225	350	-	-		107	4114
A2C78	ACT II	892	255	95	80	-	78	2992
A2C96		1102	315	125	95	-	96	3667
A2C107		1225	350	160	95	-	107	3973
A2C96N		1102	315	125	95	-	96	959

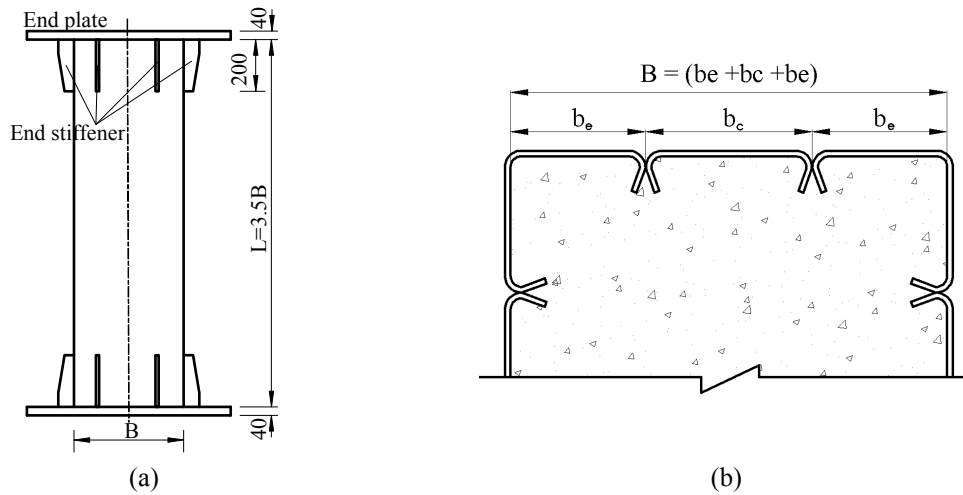


Fig. 3 Shape of specimen

The specimens are grouped into regular CFT, ACT I and ACT II columns based on the number of the stiffeners. A non-filled ACT II column (A2C96N) was also fabricated to compare the composite effect of ACT II columns. The column was fabricated from the steel plate with a thickness of 3.2 mm, which is slightly thinner than others based on the width-thickness ratio of as much as 100. The thickness of the steel plates was constant, while their widths varied to produce different width-thickness ratios. In order to minimize the influence of overall buckling, the length of the specimens was decided to be 3.5 times of the width. The single-digit numbers in specimen names show the number of the stiffeners. Columns with '0' in their names are regular CFT columns and those with '2' are ACT II columns. The two-digit numbers tell width-thickness ratios. 'N' after the two-digit number means the column is not filled with concrete. Fig. 3 shows the shape of the specimens.

In order to prevent the unbalanced load at the ends of the specimens and local buckling caused by it, 20 mm-thick end plates and 9 mm-thick rib plates were placed at the ends of the specimens. A hole (D: 150 mm) for concrete-filling was made at the upper end plate of each specimen. In addition, holes (@20) were made at the four edges of the plate to send out steam during concrete-curing.

## 2.2 Test set-up

The test in this study was conducted at the Structural Test Lab of RIST (Research Institute of Industrial Science & Technology in Korea) using a 10,000 kN UTM. Compressive monotonic loading at a speed of 0.05 mm/s was applied until load capacity fell to 80~60% of maximum load capacity after the specimens experienced maximum load. Then, the test was terminated depending on the strain speed and condition of each specimen. Loading equipment is bolt joined to the upper plate (20 mm). Both materials (steel tube and concrete) were set to load transfer at the time.

## 2.3 Results of material test

ASTM E08/E8M-11 sub-size specimens were used for material test. As shown in Table 2, yield



Fig. 4 Test set-up

Table 3 Material test result

No.	Thickness (mm)	Width (mm)	Section size (mm <sup>2</sup> )	Modulus of elasticity (GPa)	Yield strength (MPa)	Tensile strength (MPa)	Yield ratio	Elongation (%)
3.2t_A	3.00	24.93	74.88	190	341	426	0.80	31%
3.2t_B	3.01	24.68	74.46	198	353	447	0.79	33%
3.2t_C	3.01	24.93	74.80	200	357	452	0.79	30%
MEAN	3.01	24.85	74.71	196	350	440	0.79	31.3%

Table 4 Concrete compressive strength test result (D:100, L:200mm)

No.	Section size (mm <sup>2</sup> )	Compressive strength (MPa)	Modified strength (MPa)
1	7850	42.14	40.87
2	7850	46.55	45.15
3	7850	37.70	36.57
4	7850	43.16	41.86
5	7850	41.10	39.87
MEAN	7850	42.13	40.87

strength and tensile strength of 3.2 mm steel were 350 MPa and 440 MPa, respectively. And, concrete compressive strength was found to be 41 MPa as shown in Table 3.

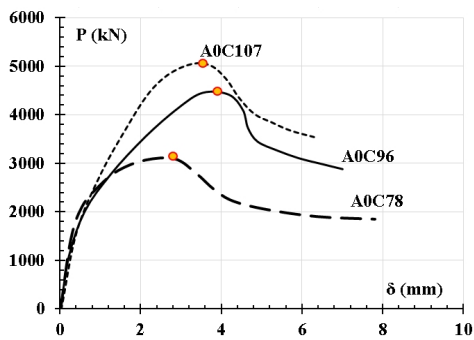
### 2.4 Experimental results

Fig. 5 shows load-displacement relationship of the specimens obtained from the average of the axial displacement measured at two opposite sides. Table 4 summarizes initial stiffness ( $K_i$ ), maximum load capacity ( $P_u$ ) and maximum displacement ( $\delta_u$ ) of the specimens. The initial stiffness ( $K_i$ ) of specimens is an inclination from 0 to  $P_u/3$ .

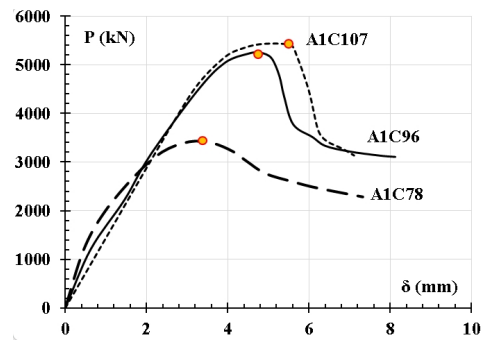
As observed in the load-displacement relationship of regular CFT specimens shown in Fig. 5(a), larger width and section size were associated with greater compressive load capacity. Initial stiffness and the behavior after maximum load capacity were similar among the specimens. As shown in Fig. 5(b), ACT I specimens displayed superior axial load capacity compared with regular

Table 5 Structural test result

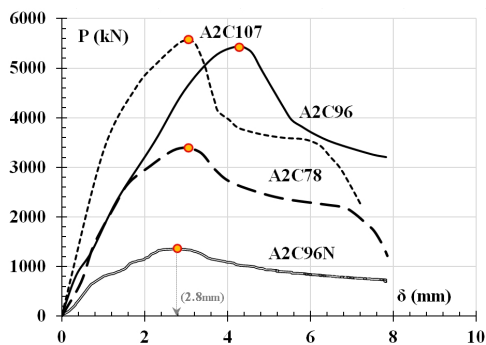
Specimen	$K_i$ (kN/mm)	$P_y$ (kN)	$P_u$ (kN)	$\delta_u$ (mm)
A0C78	509	2,386	3,182	3.91
A0C96	571	3,853	4,534	3.95
A0C107	548	4,321	5,084	3.52
A1C78	600	2,904	3,417	3.76
A1C96	601	4,464	5,252	4.36
A1C107	726	4,726	5,454	4.83
A2C78	886	2,910	3,431	3.35
A2C96	1811	4,642	5,441	4.23
A2C107	1220	4,730	5,565	2.89
A2C96N	700	1,108	1,353	2.85



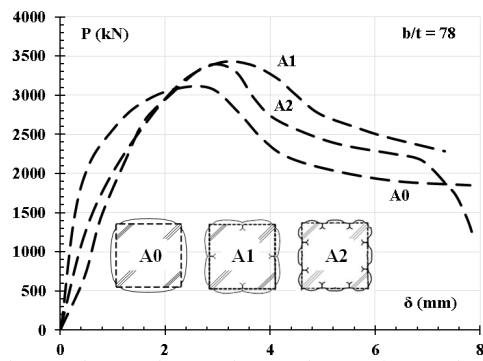
(a) CFT column



(b) ACT I



(c) ACT II



(d)  $b/t = 78$

Fig. 5 Load-displacement relationship

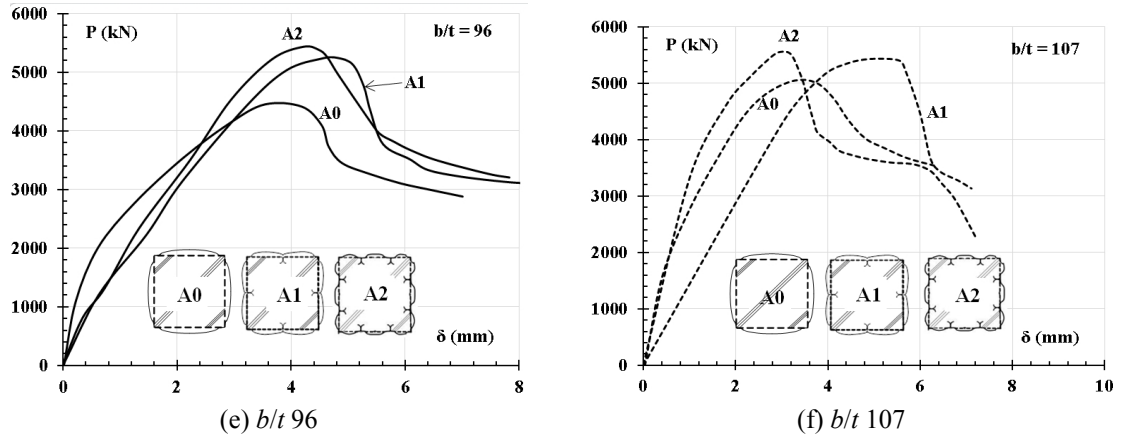


Fig. 5 Continued

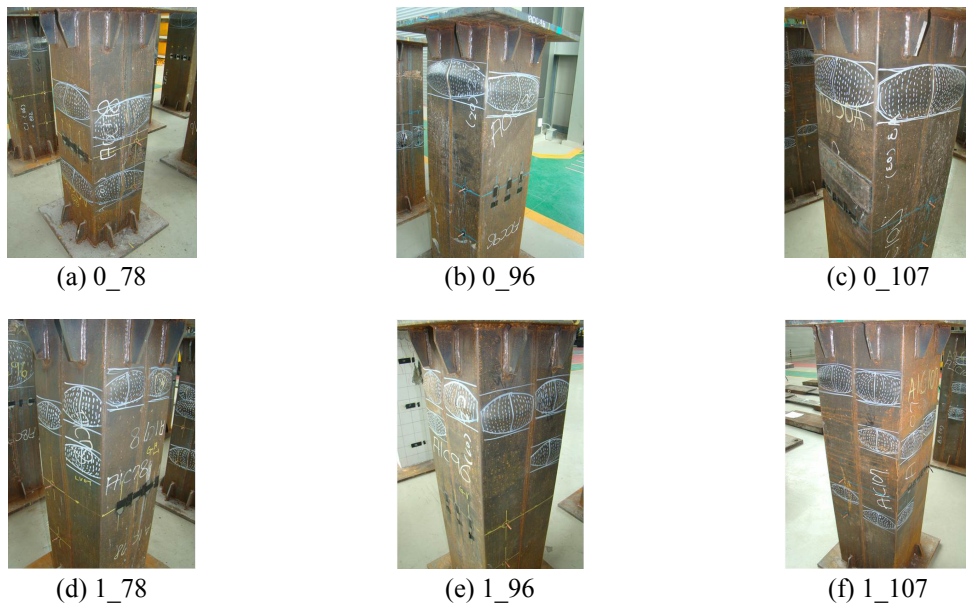


Fig. 6 Failure modes of regular CFT specimens and ACT I specimens



Fig. 7 Failure modes of ACT II and non-filled ACT II specimen

CFT specimens. The specimen having the smallest width-thickness ratio showed the most gradual behavior after maximum load capacity.

### 2.5 Failure modes

Failure modes differed among the specimen groups and depending on whether the columns were filled with concrete or not. For regular CFT specimens, outward buckling generated at the center or 1/4 point of column length was followed by rupture. In ACT I specimens, outward buckling was observed at the ends of the ribs placed at the both ends of the columns to prevent stress concentration. It was also generated at the center of the columns. Local buckling at the two sides centering around the ribs indicates that they provided anchor effect. As shown in Fig. 6, the manifestation of local buckling differed among the ACT II specimens. Buckling started at the ends of the stiffeners placed to prevent stress concentration at the upper parts of the columns.

In the ACT II specimen which was not filled with concrete, buckling was generated at the center of the column and extended to both directions covering the half of the column. In addition, in-plane and outward buckling was observed sporadically. Load capacity deteriorated rapidly after the buckling.

## 3. Analysis and implication

The following is the analysis of the structural test result of the composite columns associated with concrete-filling/non-filling, number of stiffeners and width-thickness ratio.

### 3.1 The efficiency of column sections

To investigate the effectiveness of the cross-section for ACT columns, the sectional strength given in Eq. (1), known as the squash load, was used and compared to the experimental results. It was thought that it would be possible to compare the sectional strength without considering the length effect to the member strength from experimental results, since all the specimens in this paper were very short columns for which sectional strength was almost identical to the member strengths. Eq. (1) assumes that all the cross-sections of steel are effective. Therefore, there are ineffective areas when the experimental value  $P_u$  is less than  $P_0$  computed by Eq. (1). Table 5 shows the analysis of load capacity deterioration associated with the increase in width-thickness ratio. And, the load capacity excluding the additional strength associated with the stiffeners was divided by the section strength equation ( $P_{no}$ ) as shown in Eq. (3). In Table 5  $A_{ss}$  means area of stiffener (A pair of stiffener area is 86.14 mm<sup>2</sup>). Eq (2) in Table 5 shows the results obtained from the test and the design equation and non-dimensionalized comparison of the two. As shown in the table, the test data were higher than designed values in general. Plus, In Eq. (3) while the numbers around 0.9~1 were obtained from regular CFT specimens, those from ACT I and II specimens were more than 1 indicating high in-plane efficiency. As a result, they were evaluated to be section-efficient. Since load capacity ratio was more than 1.0 despite the width-thickness ratio exceeding the code, it can be deduced that deterioration in load capacity caused by local buckling is not an issue associated with the stiffeners. Moreover, Maximum strength ( $P_u$ ) of concrete-filled specimens A2C96 was 4 times higher than the hollow specimen (A2C96N) having the same loading axis.

Table 6 Load capacity verification

Name	b/t ( bc/t )	A <sub>s</sub> (mm <sup>2</sup> )	A <sup>c</sup> (mm <sup>2</sup> )	A <sub>ss</sub> (mm <sup>2</sup> )	P <sub>u</sub> (kN)	Eq. (2)	Eq. (3)
AOC78	78	3223	61802	0	3,182	1.15	0.97
AOC96	96	3991	95234	0	4,534	1.29	0.96
AOC107	107	4439	118061	0	5,084	1.24	0.90
A1C78	78 (38)	3223	61374	344.56	3,417	1.20	1.01
A1C96	96 (47)	3991	94806	344.56	5,252	1.47	1.09
A1C107	107 (53)	4439	117633	344.56	5,454	1.34	0.96
A2C78	78 (30)	3223	60932	689.12	3,431	1.14	0.96
A2C96	96 (39)	3991	94364	689.12	5,441	1.48	1.09
A2C96N	96 (39)	3991	0	689.12	1353	1.41	0.80
A2C107	107 (50)	4439	110108	689.12	5,565	1.37	0.97

$$\frac{P_u}{P_u(\text{Eq. (1)})} \tag{2}$$

$$\frac{P_u}{A_s F_y + 0.85 A_c f_{ck} + A_{ss} F_y} \tag{3}$$

### 3.2 Rib effect

Unlike regular CFT specimens, ACT I and II specimens had ribs inside the planes. Thus, it is necessary to find what percentage of the total area the ribs cover. In ACT I specimens, steel ( $A_s + A_{ss}$ ) and ribs ( $A_{ss}$ ) comprise approximately 6.5% and 2% of the total area ( $A_g$ ), respectively. In ACT II specimens, steel and ribs comprise 7.5% and 3%. In order to analyze the consequences of ribs, tensile force which could be generated from them was evaluated. As shown in Fig. 8, the area of concrete rupture was calculated as the sum of shearing resistance at two sides (A) and tensile resistance at rib ends (B). The horizontal distance between the ribs was used as the vertical length for calculating concrete resistance area. It was assumed that the rib resistance for preventing local buckling at plates was equivalent to 2 % of the maximum force applied to the plate section.

Eqs. (4) and (5) are for calculating tensile resistance and shearing resistance, respectively. Concrete compressive strength and steel yield strength obtained from the material test were used.  $b$  and  $d$  were constant in all of the specimens as shown in Fig. 8, while effective rib width  $s$  and axial length ( $h = S$ ) varied depending on the overall width of the column as shown in Fig. 8. In ACT I specimens,  $S$  or  $h$  was 1/2 of total width. Here,  $0.42(f_{ck})^{0.5}$  means tensile strength of concrete and  $f_{ck}^{0.5}/6$  is Shear strength of concrete.

(1) Tensile resistance

$$\phi f_t = \phi 0.42 \sqrt{f_{ck}} (bh) \quad (\phi = 0.55) \tag{4}$$

(2) Shearing resistance

$$\phi V_s = \phi \frac{\sqrt{f_{ck}}}{6} (dh) \quad (\phi = 0.75) \tag{5}$$

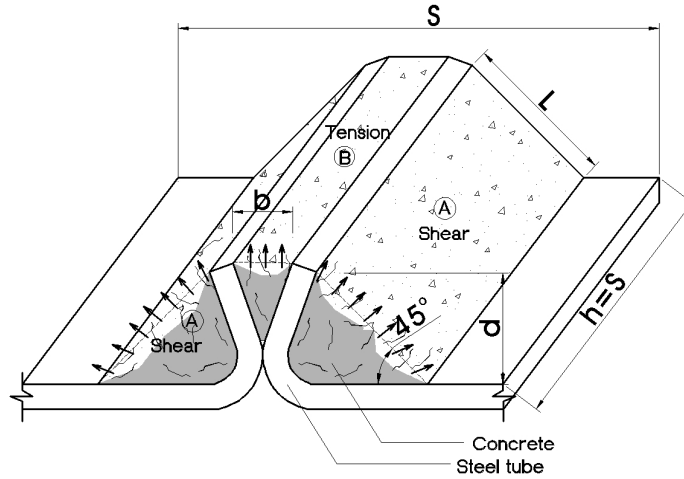


Fig. 8 Area of concrete rupture caused by ribs

Table 7 Buckling and tensile resistance of ribs

Name	'A' Tensile (N)	'B' Shearing (N)	'C' (A + B) × rib of number	'D' Buckling resistance load (N)	Load ratio (D/C)
A1C78	3,121	5,295	33,666	18,597	0.6
A1C96	3,856	6,541	41,588	23,435	0.6
A1C107	4,284	7,268	46,209	26,258	0.6
A2C78	2,142	3,634	46,209	17,152	0.4
A2C96	2,693	4,568	58,091	21,991	0.4
A2C107	3,121	5,295	67,333	24,813	0.4

## (3) Maximum load capacity and buckling resistance load of plate section

$$\phi P_{ns\_max} = \phi A_s F_y \times 0.02 \quad (\phi = 0.90) \quad (6)$$

Table 6 shows resistance and buckling resistance load of ACT I and II specimens obtained from Eqs. (4)~(6). Buckling resistance load of plate section was set to be 2% of the maximum load applied to it. Load ratio was calculated by dividing buckling resistance load by resistance (tensile + shearing). The result shows that the ribs provided enough anchor effect for the buckling resistance load of the plates.

## 4. Field application

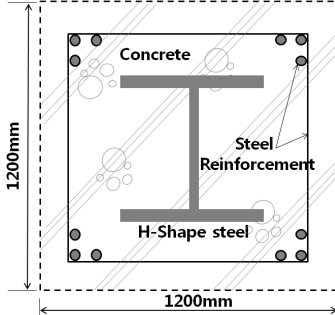
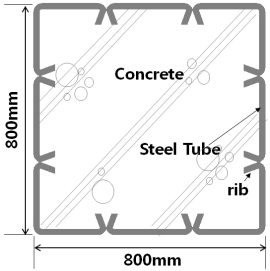
### 4.1 Outline

ACT columns were employed in the refrigerated warehouse with 2 stories below and 4 above

Table 8 Outline of field application

Bird's-eye view		Title	OO Cold storage New Construction
		Location	Gyeonggi-do in Korea
		Lot area	8,120 m <sup>2</sup>
		Use	Low Temperature Storage-
		Scale	14,040 m <sup>2</sup> (4 stories above ground 2 underground levels)
		Structure type	Steel-frame structure, RC structure
Col. Type	ACT I	Ground 1~4 F: □ – 616×616×10	
		Underground 2~Ground 4F: □ – 566×566×10	
	ACT II	Underground 2F: □ – 800×800×10	

Table 9 Cross- sectional size

H-SRC Col.	ACT II Col.
	

the ground shown in Table 4. Used to store agricultural, forestry, fishery and livestock products, the warehouse has refrigerators and freezers. It also has a large parking place for users' convenience. Therefore, it was planned as a long-span structure under heavy vertical axial loads. ACT I columns were employed in both below and above the ground. ACT II columns were employed in the central parts of basements subject to the heaviest axial load.

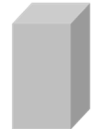
Since factory-manufactured ACT steel tubes were used in construction field, term of works and construction process were not influenced. As mentioned above, ACT columns with ribs present higher cross-sectional efficiency and smaller cross-sections when compared with generic square columns. In addition, relatively thin steel plates can be used. Therefore, relatively large space was available after the columns were placed. If SRC columns are used, steel bars, molds and equipment should be placed and the serviceability of the structure is reduced due to the larger cross-sectional size of the columns. As shown in Table 8, the width of a SRC column is 1200 mm, while that of an ACT II column dealing with the same axial load is 800 mm.

#### 4.2 Benefits

Comparison with the warehouses employing Normal CFT, FH-shaped, SRC and PC columns

verified the structural safety of the structure employing ACT I and ACT II columns as mentioned in chapter 3. Both ACT I and ACT II columns provide benefits in terms of fabric-ability and workability and the latter surpass the former in flexibility and structural safety. Although ACT II columns have larger width-thickness ratio when compared with ACT I columns, the 8 ribs of the former delay local buckling and provide high load capacity. Therefore, they can be employed in warehouses or factories with high floor height and working load. ACT columns are superior in terms of economic efficiency because one ACT column covers larger floor area in a high-rise building thanks to its excellence in structural performance and cross-sectional efficiency. Table 10 is the comparison of construction cost. When compared with ACT I columns, CFT columns, H-shaped columns, SRC columns and PC columns cost 2.29, 1.23 and 1.18 times, respectively.

Table 10 Comparison of construction cost

Type	Section size	Cost of Construction / 1m					Ratio (%)	
		Case	Quantity	Unit	Cost (\$)	Sum (\$)		
 ACT Col.	□ – 618×618×10.5	ACT col.	0.277	kg	1718.72	476.08	<b>100</b>	
		HD32	0.125	kg	893.73	111.72		
		Con’c	0.38	m <sup>3</sup>	98.21	37.32		
		Intumescent paint	2.47	m <sup>2</sup>	34.37	84.9		
		<b>Sum</b>				<b>710.015</b>		
 CFT Col.	□ – 618×618×15	CFT Col	0.356	kg	2096.83	733.89	<b>136%</b>	
		HD32	0.125	kg	893.73	111.72		
		Con’c	0.37	m <sup>3</sup>	98.21	37.32		
		Intumescent paint	2.47	m <sup>2</sup>	34.37	84.9		
		<b>Sum</b>				967.82		
 H- Col.	H – 650×650×40×60	H-COL	0.782	kg	1669.61	1305.64	<b>201%</b>	
		Intumescent paint	3.6	m <sup>2</sup>	34.37	123.75		
		<b>Sum</b>				<b>1429.39</b>		
 SRC Col.	H – 428×407×20×35 RC-900×900	H-Col.	0.283	kg	1522.29	430.81	<b>108%</b>	
		HD22	0.059	kg	991.95	58.52		
		Con’c	0.81	m <sup>3</sup>	59791	48.53		
		Form	3.6	m <sup>2</sup>	58.93	212.14		
		Finish	3.6	m <sup>2</sup>	4.91	17.68		
		<b>Sum</b>				<b>767.68</b>		
 PC Col.	□ – 1000×1000	Con’c	1	m <sup>3</sup>	736.59	736.59	<b>104%</b>	
		<b>Sum</b>				<b>736.59</b>		

\* If, (1) Axial Load: 1860 Ton; (2) Floor height: 10.4 m; (3) Span: 11 × 11 m;  
(4) Include steel production costs

While the width of column or the number of columns increases when SRC columns or PC columns are used, the cost does not increase as much as in H-shaped columns because fireproofing painting is not mandatory. However, cost increase would be larger if space availability and connection were taken into consideration.

## 5. Conclusions

This study presented a new shape of steel tube, the ACT tube, to be used as a new scheme of stiffened CFT, called ACT-CFT. ACT tube does not require an additional process for installation of stiffeners, since the ribs in ACT tube that act as stiffeners are already installed during the production of ACT tube. The conclusion obtained from the test of ten specimens to evaluate the structural performance and behavior of new shape built-up square stub CFT columns under axial Loading and theoretical analysis based on the test is as follows:

- ACT II specimens were proved to secure enough load capacity in spite of their width-thickness ratios being greater than what is prescribed in design code and thus, have improved sectional efficiency.
- The comparison between the tensile force generated from the anchor effect and buckling strength was conducted to analyze the influence of the ribs of ACT I and II specimens which comprised 2~3% of total area. The maximum tensile force of the ribs was found to be greater than buckling strength. The dimensions of the specimens were scaled down due to the capacity of the test equipment and the ribs with a length of 20 mm were used in the specimens. While the anchor effect was not great because 20 mm was not long enough, the employment of 50 mm-long ribs as in actual structures would have enabled them to generate enough anchor effect.
- The comparison between section strength and test result showed that the anchor effect provided by the ribs improved the load capacity of the specimens though the width-thickness ratios exceeded the limit prescribed in the design code.
- That ACT columns have excellent structural performance and cross-sectional efficiency and thus the floor area one ACT column covers in a high-rise building is larger makes both ACT I and ACT II columns cost-efficient and desirable.

## References

- AISC (2005, 2010), *Steel Construction Manual*, American Institute of Steel Construction Inst.
- Bahrami, A., Wan Badaruzzamana, W.H. and Osman, S.A. (2011), "Nonlinear analysis of concrete-filled steel composite columns subjected to axial loading", *Struct. Eng. Mech., Int. J.*, **39**(3), 383-398.
- Eurocode 4 (2004), Design of composite steel and concrete structures; EN 1994-1-1:2004, European Committee for Standardization.
- Fujimoto, T., Mukai, A., Nishiyama, I. and Sakino, K. (2004), "Behavior of eccentrically loaded concrete-filled steel tubular columns", *J. Struct. Eng.*, **130**(2), 203-212.
- Furlong, R.W. (1967), "Strength of steel-encased concrete beam columns", *J. Struct. Div.*, **93**, 113-124.
- Hajjar, J.F. and Gourley, B.C. (1996), "Representation of concrete-filled steel tube cross-section strength", *J. Struct. Eng.*, **122**(11), 1327-1336.
- KBC (2005, 2009), Korean Building Code; *Architectural Institute of Korea*.
- Lee, S.H., Yang, I.S. and Choi, S.M. (2010), "Structural characteristics of welded built-up square CFT

- column-to-beam connections with external diaphragms”, *Steel Compos. Struct., Int. J.*, **10**(3), 711-722.
- Lee, S.H., Kim, S.H., Kim, Y.H., Tao, Z. and Choi, S.M. (2011), “Water-pressure test and determination of welding-throat-depth for welded built-up square CFST column”, *J. Construct. Steel Res.*, **67**(7), 1065-1077.
- Park, R. and Paulay, T. (1933), *Reinforced Concrete Structures*, A Wiley – Interscience Publication; John Wiley & Sons.
- Schneider, S.P. (1998), “Axially loaded concrete-filled steel tubes”, *J. Struct. Eng.*, **124**(10), 1125-1138.
- Tomii, M. and Sakino, K. (1979), “Elasto-plastic behavior of concrete filled square steel tubular beam-columns”, *Transact. Architect. Inst. Japan*, **280**, pp. 111-120.
- Uy, B. and Bradford, M.A. (1996), “Elastic local buckling of steel plates in composite steel-concrete members”, *Eng. Struct.*, **18**(3), 193-200.
- Xiamuxi, A. and Hasegawa, A. (2011), “Compression test of RCFT columns with thin-walled steel tube and high strength concrete”, *Steel Compos. Struct., Int. J.*, **11**(5), 391-402.

BU